

Numerical Analysis for Prediction of Fatigue Crack Opening Level

Hyeon Chang Choi*

Department of Mechatronics Engineering,
College of Engineering, TongMyong University of Information Technology,
535 Yongdang-dong, Nam-gu, Busan 608-711, Korea

Finite element analysis (FEA) is the most popular numerical method to simulate plasticity-induced fatigue crack closure and can predict fatigue crack closure behavior. Finite element analysis under plane stress state using 4-node isoparametric elements is performed to investigate the detailed closure behavior of fatigue cracks and the numerical results are compared with experimental results. The mesh of constant size elements on the crack surface can not correctly predict the opening level for fatigue crack as shown in the previous works. The crack opening behavior for the size mesh with a linear change shows almost flat stress level after a crack tip has passed by the monotonic plastic zone. The prediction of crack opening level presents a good agreement with published experimental data regardless of stress ratios, which are using the mesh of the elements that are in proportion to the reversed plastic zone size considering the opening stress intensity factors. Numerical interpolation results of finite element analysis can precisely predict the crack opening level. This method shows a good agreement with the experimental data regardless of the stress ratios and kinds of materials.

Key Words : Fatigue Crack Growth, Finite Element Analysis, Crack Closure Behavior, Prediction of Opening Level, Reversed Plastic Zone Size

Nomenclature

Δa : Element size on crack surface
 Δa_{ini} : Initial crack size
 Δa_{fin} : Final crack size
 H' : Linear strain hardening rate
 k : Correction factor
 ΔK : Stress intensity factor range
 ΔK_{eff} : Effective stress intensity factor range
 K_{op} : Crack opening stress intensity factor
 ΔL : Stress range
 R : Stress ratio
 ν : Poisson's ratio
 Δr_p : Reversed plastic zone size

σ_{op} : Crack opening stress
 σ_y : Yield stress
 ΔS_{eff} : Effective stress ranges
 S_{max} : Maximum stress
 S_{cl} : Crack closing stress
 ΔS : Load range
 U : Effective stress intensity factor range ratio
 U_{assume} : Assumed effective stress intensity factor range ratio
 U_{cal} : Calculated effective stress intensity factor range ratio

* E-mail : hcchoi@tit.ac.kr

TEL : +82-51-610-8354; FAX : +82-51-610-8349

Department of Mechatronics Engineering, College of Engineering, TongMyong University of Information Technology, 535 Yongdang-dong, Nam-gu, Busan 608-711, Korea. (Manuscript Received May 25, 2004; Revised August 6, 2004)

1. Introduction

Finite element analysis is the most popular numerical method to simulate plasticity-induced fatigue crack closure (Newman, 1976, 1977; Ohji et al., 1974). Recently Solanki et al. (2004)

said that the issues concerning the most two-dimensional analyses have become reasonably well understood from their review paper. But there are few studies that made comparisons between finite element method and experimental results.

According to the studies of Choi and Song (1995), Park et al. (1997) and McClung and Sehitoglu (1991), the crack growth phenomenon through the numerical analysis is simulated as releasing a node along the crack line when a nodal reaction force changes from tension to compression force. The valid crack opening level is obtained when it becomes stable after the crack tip advances beyond the monotonic plastic zone induced by the initial crack length. The monotonic plastic zone, the region of material experiencing plastic deformation when the cracked member is subject to the maximum load in the cycle, is defined for plane stress conditions as follows

$$r_p = \frac{1}{\pi} \left(\frac{K_{\max}}{\sigma_y} \right)^2 \quad (1)$$

McClung (1991) developed a simple method to predict the reversed plastic zone size in fatigue which takes crack closure into account. The basic concept is a simple one. Reversed plastic flow at the crack tip is driven by a singular stress field as long as the crack tip is open. When the crack tip closes, the singularity vanishes, but some further reversed plasticity can occur due to nominal applied stresses. The size of the reversed plastic zone at the moment of first crack tip closure is given by

$$\Delta r_p = \frac{1}{\pi} \left(\frac{\Delta K_{\text{eff}}}{2\sigma_y} \right)^2 \quad (2)$$

where effective stress intensity factor ranges $\Delta K_{\text{eff}} = \Delta S_{\text{eff}} \sqrt{\pi a}$ and effective stress ranges $\Delta S_{\text{eff}} = S_{\max} - S_{\text{cl}}$.

Choi (2000, 2003) showed that the prediction of crack opening level presents a good agreement with the experiment data regardless stress ratios, which uses the mesh of elements that are in proportion to the reversed plastic zone size

calculated by the opening stress intensity factors. But the weak point of this method is that the opening stress level is needed for the determination of the mesh sizes that are in proportion to the reversed plastic zone size.

Based on the previous researches, this paper is going to carry out the prediction of crack opening level that is determined by numerical interpolation using the assumed K_{op} calculated by the reversed plastic zone size through FEA. The advanced prediction method of crack opening level will be proposed.

2. Finite Element Model for the Prediction of Crack Closure Model

The detailed finite element model was shown in the author's previous work (Choi, 2000). A comparison between numerical and experimental results is very important to derive quantitative conclusions from finite element method. Therefore, we developed the same model for numerical analysis as the experimental specimen. A center-cracked tension (CCT), of initial notch $2a_0 = 16$ mm, 10 mm thick, 184 mm long and 70 mm wide, is used as a finite element model for numerical analysis. Four-node isoparametric elements are used (Owen and Fawke, 1983). Only one-quarter of the specimen is modelled.

Figure 1 shows the typical fine mesh configuration near crack tip surface. In this study, the sizes of elements in the fine mesh zone along the crack line linearly increase as shown in the previous work (Choi, 2000).

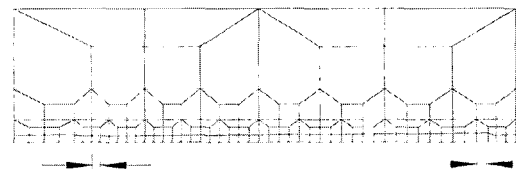


Fig. 1 Typical increasing fine mesh along crack line used in this study

3. Results of Crack Opening Behavior Prediction

From the Eq. (2) we can derive as

$$U = \frac{\sqrt{\pi} \Delta r_p (2\sigma_y - \Delta S)}{\Delta K - \Delta S \sqrt{\pi} \Delta r_p} \quad (3)$$

where U is the effective stress intensity factor range ratio, which is the function value determined by stress intensity factor range, applied load range and reversed plastic zone size. Eq. (3) represents that the effective stress range ratio U has the relationship with Δr_p . The below formula can be deduced.

$$\Delta r_p \propto \left(\frac{U \Delta S \sqrt{\pi a}}{2\sigma_y - (1-U) \Delta S} \right)^2 \quad (4)$$

$\Delta S = \sigma_y \Delta L$ is applied to Eq. (4)

$$\Delta r_p \propto \left(\frac{U \sqrt{\pi a}}{\frac{2}{\Delta L} - (1-U)} \right)^2 \quad (5)$$

where ΔL is the applied loading range and $\Delta L < 0.1$ because of high cycles fatigue, U is always less than 1. Eq. (6) can be derived.

$$\Delta r_p \propto (U \sqrt{\pi a} \Delta L)^2 \quad (6)$$

It can be assumed that applied loading range and crack length are constant regardless stress ratio. Eq. (7) can be shown as

$$\Delta r_p \propto U^2 \quad (7)$$

This relationship shows that the reversed plastic zone size is proportional to the power of effective stress intensity range ratio. Generally, it is reported that U is represented as the function of R like Eq. (8). Therefore the reversed plastic zone size is the function of R .

$$U \propto f(R) \quad (8)$$

$$\Delta r_p \propto f(R)^2 \quad (9)$$

From the above equations we can know that the reversed plastic zone size is determined by R when applied loading range and crack length are constant. U is determined for any stress ratio from Eq. (3).

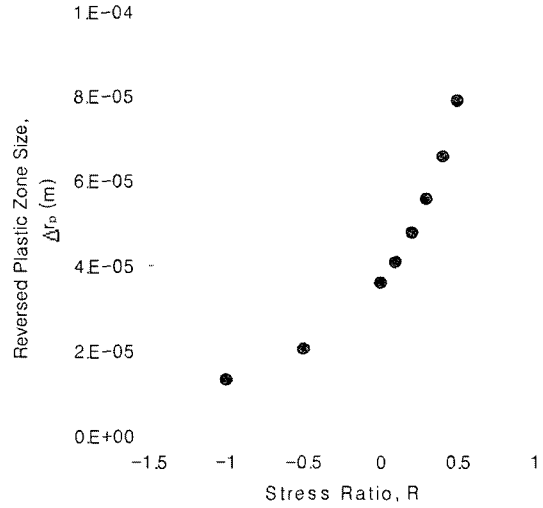


Fig. 2 Reverse plastic zone size for various stress ratios

Figure 2 shows the reversed plastic zone size calculated by U from the crack opening results of Kurihara et al.'s experiment. Material used for Kurihara et al.'s experiment is structural steel JIS SM50B. Material properties are follows: Young's modulus $E=200$ GPa, Poisson's ratio $\nu=0.3$, yield stress $\sigma_y=367$ MPa, and the plastic modulus or the linear strain hardening parameter $H' = (d\sigma_y/d\varepsilon) = 0.01E = 2000$ MPa. The results of Kurihara et al.'s experiment represent the relationship of $U=1/(1.5-R)$. Figure 2 shows the variation of reversed plastic zone size depending on stress ratio R in case that the applied loading range and the crack length are constant. The reversed plastic zone size outstandingly increases as stress ratio R increases. The maximum and the mean loading increases in case of R increment even though the loading range is constant. Therefore the reversed plastic zone size becomes larger as a square power function of stress ratio as shown in Eq. 9. Equation (6) assumes that the element size at crack tip region is in proportion to the reversed plastic zone size, which can be shown as

$$\Delta r_p = k \Delta a \quad (10)$$

where Δa is element size at crack tip and k is proportional constant.

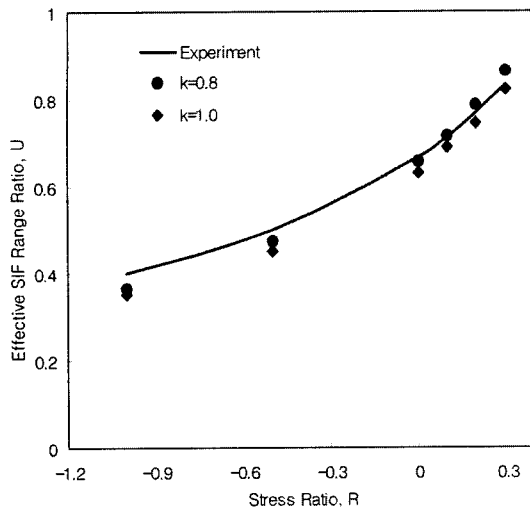


Fig. 3 Effective stress intensity factor range ratio, U , according to correction factors of element size calculated by reversed plastic zone size

Figure 3 shows the FEA results of crack opening of JIS SM50B for $k=1$ and $k=0.8$, respectively and the relationship between the stress ratio, R , and the effective stress intensity factor range ratio U . FEA result for $k=1$ indicates slightly lower than the experimental result over all R values. But $k=0.8$ is more similar to experimental data than $k=1$. In this work $k=0.8$ is used as a proportional constant.

For various comparisons we also apply to an aluminum material. The published experimental crack opening data used for the comparison is the results obtained from Kim (1993)'s experimental report. Material properties for the analysis are as follows: Young's modulus $E=70$ GPa, Poisson's ratio $\nu=0.33$, yield stress $\sigma_y=379$ MPa, and the plastic modulus or the linear strain hardening parameter $H'=(d\sigma_y/d\varepsilon)=0.01E=700$ MPa. These properties are expected to correspond to the 2024-T351 aluminium alloy. The result of proportional constant $k=0.8$ also shows the same trend for aluminum 2024-T351, which is not presented in this work. It can be deduced from the above results that the effective stress intensity range ratio solely corresponds to the stress ratio and the reversed plastic zone size such as $U=1/(1.5-R)$ for JIS SM50B.

In here, the algorithm for the effective stress

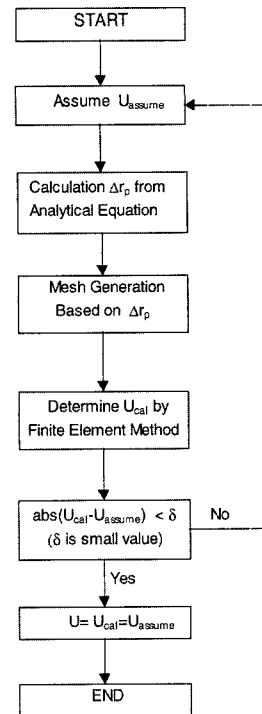


Fig. 4 Flow chart of prediction method of crack opening level

intensity range ratio, U , using FEA for the constant stress ratio is shown in Fig. 4. Firstly, the reversed plastic zone size Δr_p is determined by the assumed effective stress intensity range ratio U_{assume} using Eq. (2). The element size at crack tip is calculated using Δr_p from Eq. (10). The mesh for FEA to predict crack opening behavior is generated as the method described in the previous work (Choi, 2000; 2003). Secondly, FEA to predict crack opening behavior is carried out. The calculated effective stress intensity range ratio is determined from the results of FEA. Finally, if the difference between U_{cal} and U_{assume} is within tolerance, U value is determined. If not, U_{assume} is redefined and the above procedure is repeated.

It is very important to perform a quantitative comparison between the numerical results and the experimental ones. FEA results are compared with the results of steel and aluminium. For a steel material, the JIS SM50B's experimental results of Kurihara et al.(1987) are used. For an aluminium material, Kim's experimental result are used.

The crack opening predictions for an aluminum and a steel model are carried out according to the calculation procedure of Fig. 4. Table 1 shows the results the opening level for the aluminum alloy 2024-T351. Four times calculations are performed under the assumed U_{assume} and $\Delta\gamma_p$. This calculation needs a lot of computational times to satisfy the tolerance of the difference between U_{cal} and U_{assume} in Fig. 4.

Figure 5 shows the results to determine the true crack opening value using the least square method. In Fig. 5 solid diamond marks and solid circular marks represent the assumed and the calculated values, respectively. The junction point of two fitting line denotes the predicted crack opening value for the assumed and calculated values.

Table 1 Results of opening level for aluminum alloy 2024-T351

| $\Delta\gamma_p$ (mm) | $\sigma_{op.a}/\sigma_y$ | U_{assume} | $\sigma_{op.c}/\sigma_y$ | U_{cal} |
|--------------------------|--------------------------|--------------|--------------------------|-----------|
| 0.044 | 0.031 | 0.631 | 0.0296 | 0.648 |
| 0.045 | 0.030 | 0.643 | 0.0293 | 0.651 |
| 0.047 | 0.029 | 0.655 | 0.0288 | 0.657 |
| 0.052 | 0.028 | 0.666 | 0.0282 | 0.664 |

Aluminum, $R=0$, $\sigma_{max}/\sigma_y=0.084$, $U_{pred}=0.661$

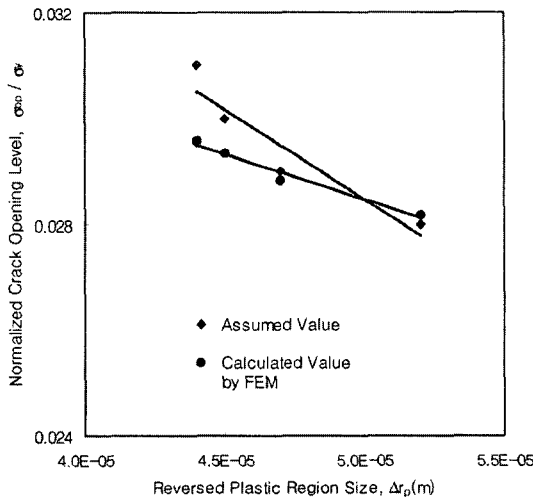


Fig. 5 Determination of opening level by least square method for aluminum alloy 2024-T351

Figure 6 shows the results of the predicted crack opening level of the aluminum alloy 2024-T351 for stress ratios $R=-1, 0.0, 0.1$ and 0.3 . A solid line indicates the experimental results by Kim (1993) and solid circular marks are the predicted crack opening level by FEA. The numerical results agree very well with experimental ones through all stress ratios.

Table 2, Fig. 7 and Fig. 8 show the results of the predicted crack opening level for the steel JIS SM50. These results also agree very well with the published experimental data as the case of the aluminum alloy 2024-T351.

From these results we can conclude that the crack opening behavior prediction using FEA and the least square method presents a good agreement with the experiment data regardless of the kinds of materials and the stress ratio. Numerical method is very useful to determine

Table 2 Results of opening level for steel JIS SM50B

| $\Delta\gamma_p$ (mm) | $\sigma_{op.a}/\sigma_y$ | U_{assume} | $\sigma_{op.c}/\sigma_y$ | U_{cal} |
|--------------------------|--------------------------|--------------|--------------------------|-----------|
| 0.03737 | 0.036 | 0.5714 | 0.03100 | 0.6310 |
| 0.03892 | 0.032 | 0.6190 | 0.03042 | 0.6379 |
| 0.04341 | 0.029 | 0.6548 | 0.02966 | 0.6469 |
| 0.04813 | 0.026 | 0.6905 | 0.02908 | 0.6538 |

Steel, $R=0$, $\sigma_{max}/\sigma_y=0.084$, $U_{pred}=0.6444$

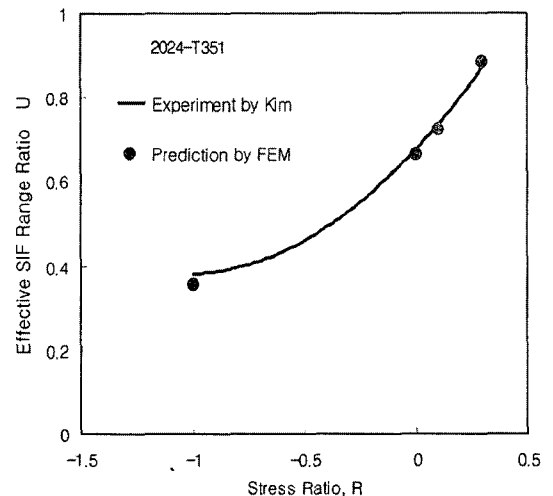


Fig. 6 Comparison between experiment and prediction for aluminum alloy 2024-T351

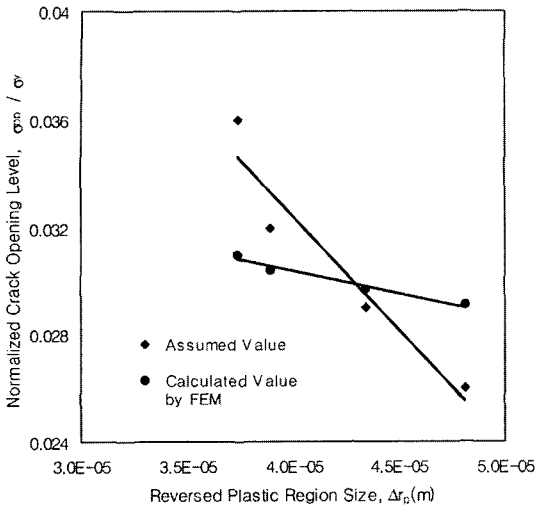


Fig. 7 Deformation of opening level by least square method for steel JIS SM50B

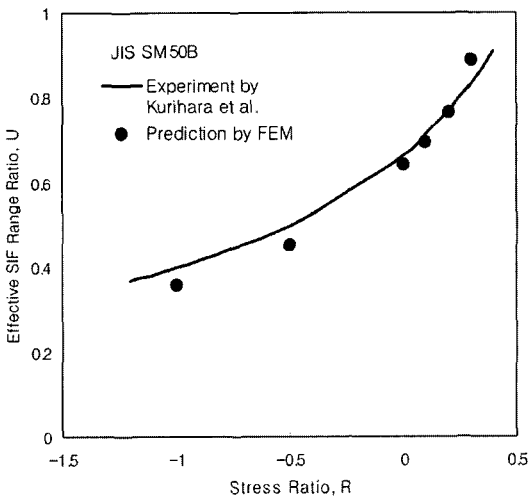


Fig. 8 Comparison between experiment and prediction for steel JIS SM50B

the crack opening level. It can be also concluded that we can precisely predict the crack opening level using only finite element method without experiment.

4. Summaries and Conclusions

The prediction method of fatigue crack opening behavior is investigated using an elastic-plastic finite element analysis. FEA using the crack tip surface mesh of elements size that are in propor-

tion to the reversed plastic zone size calculated by the opening stress intensity factors is performed for predicting crack opening level. Numerical results are compared with the experimentally measured ones. The conclusions obtained are summarized as follows:

(1) The reversed plastic zone size outstandingly increases as stress ratio R increases. The maximum and the mean loading increases in case of R increment even though the loading range is constant. Therefore the reversed plastic zone size becomes larger as a square power function of stress ratio.

(2) For the exact prediction of crack opening behavior, the element size at crack tip region varies in proportion to the reversed plastic zone size, which can be shown as $\Delta r_p = k\Delta a$. In this work the FEA result of the proportional constant, $k=0.8$, shows a good relationship with experimental result.

(3) The effective stress intensity factor range ratio, U , solely corresponds to stress ratio and reversed plastic zone size.

(4) The crack opening level predicted by using the least square method using the results of finite element analysis shows the similar results with the experiment regardless of stress ratios and materials.

(5) The crack opening level for the aluminum alloy 2024-T351 and the structural steel JIS SM50B using the method proposed in this study presents a good agreement with the experiment.

Acknowledgment

This work was supported by grant No. R05-2002-000-00167-0 from the Korea Science & Engineering Foundation and Tongmyong University of Information Technology Research Fund of 2003.

References

Choi, H. C. and Song, J. H., 1995, "Finite Element Analysis of Closure Behaviour of Fatigue Cracks in Residual Stress Fields," *Fatigue Fract.*

Engng Mater. Struct., Vol. 18(1), pp. 105~117.

Choi, H. C., 2000, "A Study on the Determination of Closing Level for Finite Element Analysis of Fatigue Crack Closure," *KSME International Journal*, Vol. 14, No. 4, pp. 401~407.

Choi, H. C., 2003, "Finite Element Analysis for Fatigue Crack Closure Behavior Using Reversed Plastic Zone Size," *J. of KSME A*, Vol. 27, No. 10, pp. 1703~1711, in Korea.

Kim, C. Y., 1993, "Fatigue Crack Closure and Growth Behavior Under Random Loading," Ph. D. Thesis, Korea Advanced Institute of Science and Technology.

Kurihara, M., Katoh, A. and Kawahara, M., 1987, "Effective of Stress Ratio and Step Loading on Fatigue Crack Propagation Rate," *Current Research on Fatigue* (Edited by Tanaka, T, Jono M, Komai K.), Elsevier Applied Science, pp. 247~265.

McClung, R. C. and Sehitoglu, H., 1989, "On the Finite Element Analysis of Fatigue Crack Closure -1. Basic Modeling Issues," *Engng Fract. Mech.*, 33, pp. 237~252.

McClung, R. C. and Sehitoglu, H., 1989, "On the Finite Element Analysis of Fatigue Crack Closure -2. Numerical Results," *Engng Fract. Mech.*, 33, pp. 253~272.

McClung, R. C., 1991, "Crack Closure and Plastic Zone Sizes in Fatigue," *Fatigue Fract. Engng Mater. Struct.*, 14(4), pp. 455~468.

Newman, Jr., J. C., 1976, "A Finite-Element Analysis of Fatigue Crack Closure," *Mechanics of Crack Growth, ASTM STP 590*, pp. 280~301.

Newman, Jr., J. C., 1977, "Finite-Element Analysis of Crack Growth Under Monotonic and Cyclic Loading," *Cyclic Stress-Strain and Plastic Deformation Aspects of Fatigue Crack Growth, ASTM STP 637*, pp. 56~80.

Ohji, K., Ogura, K. and Ohkubo, Y., 1974, "On the Closure of Fatigue Cracks Under Cyclic Tensile Loading," *Int. J. Fract.*, 10, pp. 123~134.

Owen, D. J. R. and Fawkes, A. J., 1983, *Engineering Fracture Mechanics: Numerical Method and Application*, Pineridge Press Limited Swansea, U. K.

Park, S. J., Earmme, Y. Y. and Song, J. H., 1997, "Determination of the Most Appropriate Mesh Size for a 2-d Finite Element Analysis of Fatigue Crack Closure Behaviour," *Fatigue Fract. Engng. Mater. Struct.*, Vol. 20(4), pp. 533~545.

Rice, J. R., 1967, "Mechanics of Crack Tip Deformation and Extension by Fatigue," *Fatigue Crack Propagation ASTM STP 415*, pp. 247~309.

Solanki, K., Daniewicz, S. R. and Newman Jr., J. C., 2004, "Finite Element Analysis of Plasticity-Induced Fatigue Crack Closure: An Overview," *Engineering Fracture Mechanics*, Vol. 71, pp. 149~171.